Dalton Transactions

Dynamic Article Links ►

SAND2015-4828J

Cite this: DOI: 10.1039/c0xx00000x

www.rsc.org/xxxxxx

ARTICLE TYPE

On the mechanical stability of uranyl peroxide hydrates: Implications for nuclear fuel degradation

Philippe F. Weck*[a], Eunja Kim[b], and Edgar C. Buck[c]

Received (in XXX, XXX) Xth XXXXXXXXX 20XX, Accepted Xth XXXXXXXXX 20XX

DOI: 10.1039/b000000x

The mechanical properties and stability of studtite, $(UO_2)(O_2)(H_2O)_2{\cdot}2H_2O$, and metastudtite, $(UO_2)(O_2)(H_2O)_2$, two important corrosion phases observed on spent nuclear fuel exposed to water, have been investigated using density functional perturbation theory. While $(UO_2)(O_2)(H_2O)_2$ satisfies the *necessary* and *sufficient* Born criteria for mechanical stability, $(UO_2)(O_2)(H_2O)_2{\cdot}2H_2O$ is found to be mechanically metastable, which might be the underlying cause of the irreversibility of the studtite to metastudtite transformation. According to Pugh's and Poisson's ratios and the Cauchy pressure, both phases are considered ductile and shear modulus is the parameter limiting their mechanical stability. Debye temperatures of 294 and 271 K are predicted for polycrystalline $(UO_2)(O_2)(H_2O)_2{\cdot}2H_2O$ and $(UO_2)(O_2)(H_2O)_2$, suggesting a lower micro-hardness of metastudtite.

Introduction

Understanding radiolytic corrosion and dissolution of uranium dioxide (UO_2) is of tremendous importance to assess and possibly control the mobility of uranium in the environment, from either natural deposits, or nuclear reactor accidents, or long-term storage/disposal of spent nuclear fuel (SNF) in geological repositories. Studtite, $(UO_2)(O_2)(H_2O)_2{\cdot}2H_2O$, and metastudtite, $(UO_2)(O_2)(H_2O)_2$, the only known minerals containing peroxide, are among the important corrosion phases that may form on SNF exposed to water.[1,2,3] Previous studies have suggested that such uranyl peroxide hydrates incorporating H_2O_2 generated by α-radiolysis of water[4,5,6] may play a crucial role in the degradation of SNF.[7,8,9]

The mineral studtite was originally described by Vaes,[10] and subsequently characterized in more details by Walenta[11] using chemical and powder X-ray diffraction (XRD) investigations. It was demonstrated that studtite is identical to synthetic $(UO_2)(O_2)(H_2O)_2{\cdot}2H_2O$. The fully solved structure of studtite was reported in 2003 by Burns and Hughes,[12] who showed it to be monoclinic (space group $C2/c$) with unit-cell dimensions a = 14.068(6), b = 6.721(3), c = 8.428(4) Å and β = 123.356(6)° (V = 665.6(3) Å^3; Z = 4). These authors also suggested that, in light of their structure determination for studtite and the similarity of chains of coordination polyhedra in both studtite and metastudtite, it was likely the c cell parameter previously reported by Deliens and Piret[13] for naturally occuring metastudtite was erroneous. Deliens and Piret, who proposed the name metastudtite, showed it to be equivalent to the synthetic dihydrate (a = 6.51(1), b = 8.78(2), c = 4.21(1) Å; V = 240.6(1.5) Å^3, Z = 2), first characterized by Zachariasen[14] and revised by Ukazi[15] and Debets[16]

In the absence of well-established crystallographic data for metastudtite, Ostanin and Zeller[17] proposed, on the basis of first-principles calculations, an energetically favorable orthorhombic cell with space group D_{2h}^{16} (*Pnma*) and lattice parameters a = 8.677, b = 6.803, c = 8.506 Å (Z = 4) and claimed good agreement with experimental XRD data of Deliens and Piret.[13] However, no crystallographic data for the atomic positions of this candidate structure of metastudtite were reported by Ostanin and Zeller and the computed equilibrium volume was V = 502.06 Å^3 and stated to be 4.3% larger than the experimental estimate. Using first-principles calculations, Weck *et al.*[18] proposed a model structure for $(UO_2)(O_2)(H_2O)_2$. These *ab initio* predictions were recently confirmed experimentally by Rodriguez *et al.*[19] and Guo *et al.*[20] using XRD.

The formation, thermodynamic stability, and phase transformations of studtite and metastudtite have been subjects of active research, since the presence of these alteration phases at the surface of UO_2 can significantly affect SNF dissolution rate. Sato[21] found that $(UO_2)(O_2)(H_2O)_2{\cdot}2H_2O$ precipitates below 50°C following addition of H_2O_2 to an aqueous solution containing uranyl ions, whereas $(UO_2)(O_2)(H_2O)_2$ precipitates above 70°C; a mixture of the two precipitates at 60°C. Sato demonstrated that $(UO_2)(O_2)(H_2O)_2{\cdot}2H_2O$ is converted to $(UO_2)(O_2)(H_2O)_2$ by drying in air at 100°C or in vacuum for 24 hours at room temperature. Walenta[11] also showed that, when heated to 60°C, natural studtite transforms irreversibly to metastudtite. The thermal decomposition of both phases was also studied by Cordfunke et al.[22,23] The reactivity and thermodynamic stability of these uranyl peroxide hydrates were also investigated in more details in recent studies by Hughes Kubatko et al.,[7] Rey et al.,[24] Meca et al.,[25] Mallon et al.,[26] Gimenez et al.,[27] and Guo et al.[20] In particular, Guo and co-workers were able to explain − from the thermodynamic standpoint − the irreversible transformation of studtite into metastudtite, the requirements for the formation of

metastudtite, and its significance in oxidative dissolution of SNF exposed to water.

This wealth of information on the formation, thermodynamic stability, and phase transformations of studtite and metastudtite is in stark contrast with the paucity of data regarding the mechanical stability and properties of these alteration phases formed at the SNF surface. Indeed, to the best of our knowledge, no experimental or computational studies have reported, for examples, the bulk and shear moduli, stiffness coefficients, or anisotropy factors for both phases, and the conditions of mechanical stability of studtite and metastudtite remain to be analyzed. This appears particularly surprising since the underlying atomistic deformation modes and interactions determine thermodynamic phase stability and transformation.

In this work, the mechanical properties and stability of $(UO_2)(O_2)(H_2O)_2{\cdot}2H_2O$ and $(UO_2)(O_2)(H_2O)_2$ have been systematically investigated using density functional perturbation theory. Based on the elastic constants computed in this study, the necessary and sufficient Born criteria for mechanical stability of single-crystal $(UO_2)(O_2)(H_2O)_2{\cdot}2H_2O$ and $(UO_2)(O_2)(H_2O)_2$ have been assessed. Pugh's ratio and Poisson's ratio for these materials have also been calculated for both single-crystals and polycrystalline materials within the Voigt-Reuss-Hill approximations, and the elastic parameters limiting the mechanical stability of both crystalline structures have been identified.

Details of our computational approach are given in the next section, followed by a complete analysis and discussion of our results. A summary of our findings and conclusions is presented in the last section of the manuscript.

Computational Methods

Total energy calculations were performed using the spin-polarized density functional theory (DFT) implemented in the Vienna *ab initio* simulation package (VASP).[28] The exchange-correlation energy was calculated using the generalized gradient approximation (GGA), with the parameterization of Perdew, Burke and Ernzerhof (PBE).[29] Standard functionals, such as the PBE or PW91 functionals, were found in previous studies to correctly describe the geometric parameters and properties of various uranium oxides and uranium-containing structures observed experimentally.[18,30,31,32,33] Although strong electron correlations between U(IV) 5f electrons need to be accounted for in bulk UO_2, previous studies on studtite and uranyl coordination polymers have shown that standard DFT is appropriate to describe such systems with U(VI) oxidation state[18,31]

The interaction between valence electrons and ionic cores was described by the projector augmented wave (PAW) method.[34,35] The U(6*s*,6*p*,6*d*,5*f*,7*s*) and O(2*s*,2*p*) electrons were treated explicitly as valence electrons in the Kohn-Sham (KS) equations and the remaining core electrons together with the nuclei were represented by PAW pseudopotentials. The KS equation was solved using the blocked Davidson[36] iterative matrix diagonalization scheme followed by the residual vector minimization method. The plane-wave cutoff energy for the electronic wavefunctions was set to a value of 500 eV, ensuring the total energy of the system to be converged to within 1 meV/atom. Electronic relaxation was performed with the conjugate gradient method accelerated using the Methfessel-Paxton Fermi-level smearing[37] with a Gaussian width of 0.1 eV.

In relaxation calculations, the monoclinic structure crystallizing in the space group $C2/c$ ($Z = 4$) reported by Burns and Hughes[12] was used as the starting geometry for $(UO_2)(O_2)(H_2O)_2{\cdot}2H_2O$. The orthorhombic structure of $(UO_2)(O_2)(H_2O)_2$ with space group *Pnma* ($Z = 4$), predicted from first-principles by Ostanin and Zeller[17] and Weck *et al.*[18] and confirmed experimentally with XRD by Rodriguez *et al.*[19] and Guo *et al.*,[20] was utilized as initial guess.

Ionic relaxation calculations to determine the equilibrium structures of $(UO_2)(O_2)(H_2O)_2{\cdot}2H_2O$ and $(UO_2)(O_2)(H_2O)_2$ were first carried out using the quasi-Newton algorithm and the Hellmann-Feynman forces acting on atoms were calculated with a convergence tolerance set to 0.01 eV/Å. A periodic unit cell approach was used in the calculations. Structural relaxation was performed without symmetry constraints. The Brillouin zone was sampled using the Monkhorst-Pack *k*-point scheme[38] with *k*-point meshes of 3×5×5 and 5×5×5 for studtite and metastudtite, respectively. Using the equilibrium structures obtained from total-energy minimization, successive relaxations with respect to Hellmann-Feynman forces were carried out with a convergence tolerance set to 0.001 eV/Å, and elastic properties were obtained using the linear response method, which utilizes density functional perturbation theory to calculate forces.

Results and discussion

Crystal structures

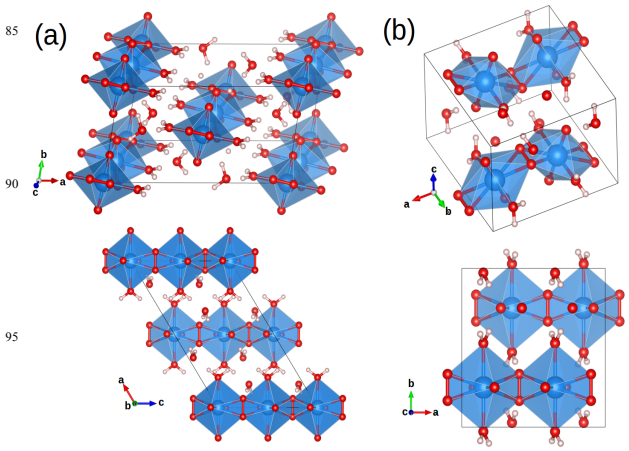

Fig. 1 Crystal unit cells of (a) $(UO_2)(O_2)(H_2O)_2{\cdot}2H_2O$ (space group $C2/c$, $Z = 4$) and (b) $(UO_2)(O_2)(H_2O)_2$ (space group *Pnma*, $Z = 4$) relaxed with DFT at the GGA/PBE level of theory. Color legend: U, blue; O, red; H, white. The uranium coordination polyhedral are shown in blue.

The crystal unit cells of $(UO_2)(O_2)(H_2O)_2{\cdot}2H_2O$ and $(UO_2)(O_2)(H_2O)_2$ relaxed with DFT are depicted in Figure 1. The equilibrium structures obtained at the GGA/PBE level of theory are consistent with previous first-principles calculations[17,18] and XRD data.[12,19,20] The relaxed structure of $(UO_2)(O_2)(H_2O)_2{\cdot}2H_2O$ is monoclinic (space group $C2/c$, $Z = 4$), with cell parameters a = 13.89, b = 6.84, c = 8.53 Å and β = 122.7° (V = 681.6 Å^3; b/a = 0.49, c/a = 0.61), i.e. in close agreement with the XRD parameters of Burns and Hughes,[12] i.e., a = 14.068(6), b = 6.721(3), c = 8.428(4) Å and β = 123.356(6)° (V = 665.6 Å^3; b/a = 0.48, c/a = 0.60). Although the equilibrium volume calculated

in this study with GGA/PBE is in slightly better agreement with experiment (i.e. +2.3% larger) than previous calculations (i.e. +3.7% larger with GGA/PBE[17] and +3.0% larger with GGA/PW91[18]), GGA calculations still overestimate bond distances and standard DFT cannot account accurately for long-range intermolecular forces between adjacent chains in the studtite structure. The relaxed structure of metastudtite crystallizes in the orthorhombic space group *Pnma* (Z = 4) with lattice parameters a = 8.46, b = 8.67, c = 6.79 Å (V = 497.6 Å^3; b/a = 1.02, c/a = 0.80), with only minute differences with previous GGA/PW91[18] predictions. The calculated volume overestimates by ~3.7% the unit cells recently solved with XRD by Rodriguez *et al.*[19] (a = 8.411(1), b = 8.744(1), c = 6.505(1) Å; V = 478.39 Å^3; b/a = 1.039, c/a = 0.773) and Guo *et al.*[20] (a = 8.4184(4), b = 8.7671(4), c = 6.4943(3) Å; V = 479.311 Å^3; b/a = 1.0396, c/a = 0.7714). Similar to studtite, this can be ascribed to some of the limitations of standard DFT/GGA methods. For this reason, the experimental lattice parameters reported by Burns and Hughes[12] for $(UO_2)(O_2)(H_2O)_2{\cdot}2H_2O$ and by Guo *et al.*[20] for $(UO_2)(O_2)(H_2O)_2$ were used in this study, rather than the relaxed lattice parameters, with limited impact on the crystal properties calculations.

Detailed discussions of the atomistic structure of $(UO_2)(O_2)(H_2O)_2{\cdot}2H_2O$ and $(UO_2)(O_2)(H_2O)_2$ were given previously.[12,17,18,19,20] As shown in Figure 1, $(UO_2)(O_2)(H_2O)_2{\cdot}2H_2O$ is made of extended chains propagating along the c axis. The ubiquitous uranyl unit is positioned with uranium on a 4*a* Wyckoff site ($\bar{1}$ symmetry) and coordinated by six equatorial oxygen atoms (on 8*f* Wyckoff sites) donated by symmetry-related pairs of water and peroxo groups. The local environment of the U metal center is hexagonal bipyramidal with two short axial U=O bonds, and a linear O=U=O angle, and with equatorial oxygen atoms. The peroxo atoms are μ^2-bridging between symmetry-related uranium metal centers. The structure of $(UO_2)(O_2)(H_2O)_2$ consists of polymeric chains propagating along the a axis (cf. Figure 1). The uranyl unit is positioned with uranium on a 4*c* Wyckoff site (.m. symmetry) and coordinated by six equatorial oxygen atoms on 8*d* Wyckoff sites donated by water and peroxo groups. The local hexagonal bipyramidal environment of the U metal center consists of two short axial U=O bonds, with a nearly linear O=U=O angle, and with equatorial oxygen atoms. The μ^2-bridging peroxo atoms have a bond distance identical to the bond distance in $(UO_2)(O_2)(H_2O)_2{\cdot}2H_2O$. Only minor differences are found between previous GGA/PW91 calculations[18] and the present GGA/PBE interatomic distances and bond angles, therefore the interested reader is referred to our previous work.[18]

Mechanical Properties

Using the structures of $(UO_2)(O_2)(H_2O)_2{\cdot}2H_2O$ and $(UO_2)(O_2)(H_2O)_2$ relaxed with respect to Hellmann-Feynman forces, elastic constants were calculated at T = 0 K as the second derivatives of the energy with respect to the strain, i.e.

$$C_{ij} = \frac{1}{V}\left(\frac{\partial^2 U}{\partial\varepsilon_i \partial\varepsilon_j}\right)$$

where V is the volume, U is the total energy of the system, and ε is the infinitesimal displacement. The Voigt notation, which relates the elastic stiffness coefficients C_{ijkl} (i, j, k, l = x, y, z) in the different directions in the crystal to the C_{ij} (i, j = 1,…, 6) elastic constants, was adopted in this study, i.e. $xx \rightarrow 1$, $yy \rightarrow 2$, $zz \rightarrow 3$, $yz \rightarrow 4$, $zx \rightarrow 5$, and $xy \rightarrow 6$. The 6×6 elasticity tensor was determined by performing six finite distortions of the equilibrium lattice and deriving the elastic constants from the strain-stress relationship.[39] The elastic behavior of $(UO_2)(O_2)(H_2O)_2{\cdot}2H_2O$ and $(UO_2)(O_2)(H_2O)_2$ single crystals is determined by 13 and 9 non-degenerate elastic constants, respectively, in the symmetric elasticity tensor C:[40]

$$C = \frac{1}{V}\left(D_{\varepsilon\varepsilon} - D_{\varepsilon i} D_{ij}^{-1} D_{j\varepsilon}\right),$$

with

$$D_{\varepsilon\varepsilon} = \left(\frac{\partial^2 U}{\partial\varepsilon\,\partial\varepsilon}\right)_{internal},$$

$$D_{\varepsilon i} = \left(\frac{\partial^2 U}{\partial\varepsilon\,\partial\alpha_i}\right)_{\varepsilon},$$

and

$$D_{ij} = \left(\frac{\partial^2 U}{\partial\alpha_i \partial\beta_j}\right)_{\varepsilon}.$$

The thirteen independent elastic constants in the stiffness matrix for the monoclinic lattice structure of $(UO_2)(O_2)(H_2O)_2{\cdot}2H_2O$ are:

$$C_{mono} = \begin{pmatrix} C_{11} & C_{12} & C_{13} & 0 & C_{15} & 0 \\ & C_{22} & C_{23} & 0 & C_{25} & 0 \\ & & C_{33} & 0 & C_{35} & 0 \\ & & & C_{44} & 0 & C_{46} \\ & & & & C_{55} & 0 \\ & & & & & C_{66} \end{pmatrix}$$

and the nine independent elastic constants for the orthorhombic lattice structure of $(UO_2)(O_2)(H_2O)_2$ are:

$$C_{ortho} = \begin{pmatrix} C_{11} & C_{12} & C_{13} & 0 & 0 & 0 \\ & C_{22} & C_{23} & 0 & 0 & 0 \\ & & C_{33} & 0 & 0 & 0 \\ & & & C_{44} & 0 & 0 \\ & & & & C_{55} & 0 \\ & & & & & C_{66} \end{pmatrix}$$

The total elastic moduli of $(UO_2)(O_2)(H_2O)_2{\cdot}2H_2O$ and $(UO_2)(O_2)(H_2O)_2$ calculated with DFPT, including both the contributions for distortions with rigid ions and the contributions from the ionic relaxations, are summarized in Table 1.

Table 1. Elastic constants (in GPa) for $(UO_2)(O_2)(H_2O)_2{\cdot}2H_2O$ and $(UO_2)(O_2)(H_2O)_2$ calculated with DFPT at the GGA/PBE level of theory.

C_{ij}	$(UO_2)(O_2)(H_2O)_2{\cdot}2H_2O$	$(UO_2)(O_2)(H_2O)_2$
C_{11}	57.0	116.7
C_{22}	31.3	56.3
C_{33}	87.4	45.5
C_{44}	7.1	18.3
C_{55}	23.4	10.2
C_{66}	10.8	13.2
C_{12}	19.9	25.1
C_{13}	28.8	32.9
C_{23}	19.8	31.5
C_{15}	-14.0	

C_{25}	-2.6
C_{35}	-19.0
C_{46}	-0.5

For low-symmetry monoclinic phases such as $(UO_2)(O_2)(H_2O)_2{\cdot}2H_2O$, a number of possible formulations of the generic Born elastic stability conditions[41,42] for an unstressed single crystal have been proposed. Popular criteria for mechanical stability are given by:[43]

$$C_{ii} > 0 \ (i = 1, \dots, 6),$$

$$C_{33}C_{55} - C_{35}^2 > 0, \qquad C_{44}C_{66} - C_{46}^2 > 0,$$

$$C_{22} + C_{33} - 2C_{23} > 0,$$

$$C_{11} + C_{22} + C_{33} + 2(C_{12} + C_{13} + C_{23}) > 0,$$

$$C_{22}(C_{33}C_{55} - C_{35}^2) + 2C_{23}C_{25}C_{35} - C_{23}^2C_{55} - C_{25}^2C_{33} > 0,$$

$$\begin{aligned} 2[C_{15}C_{25}(C_{33}C_{12} - C_{13}C_{23}) + C_{15}C_{35}(C_{22}C_{13} - C_{12}C_{23}) \\ + C_{25}C_{35}(C_{11}C_{23} - C_{12}C_{13})] - [\, C_{15}^2(C_{22}C_{33} - C_{23}^2) \\ + C_{25}^2(C_{11}C_{33} - C_{13}^2) + C_{35}^2(C_{11}C_{22} - C_{12}^2)] + gC_{55} > 0, \end{aligned}$$

with

$$g = C_{11}C_{22}C_{33} - C_{11}C_{23}^2 - C_{22}C_{13}^2 - C_{33}C_{12}^2 + 2C_{12}C_{13}C_{23}.$$

While the aforementioned conditions are fully satisfied by the elastic constants for $(UO_2)(O_2)(H_2O)_2{\cdot}2H_2O$ reported in Table 1, such criteria often proposed in the literature for single-crystal monoclinic phases are *necessary*,[44,45] but not *sufficient* criteria for mechanical stability, as recently noted by Mouhat and Coudert.[46] In particular, the generic *necessary* and *sufficient* Born criterion that all eigenvalues of the *C* matrix be positive is not satisfied, since some of the mixed elastic constants are negative, i.e. $C_{i5} < 0 \ (i = 1,2,3)$ and $C_{46} < 0$. Such mechanical metastability of $(UO_2)(O_2)(H_2O)_2{\cdot}2H_2O$ might be an underlying cause of the observed irreversibility of the dehydration transformation of studtite into metastudtite occurring at moderate temperature.[11]

For the orthorhombic $(UO_2)(O_2)(H_2O)_2$ single crystal, the *necessary* and *sufficient* Born criteria for mechanical stability are:[41,42,46]

$$C_{ii} > 0 \ (i = 1,4,5,6),$$

$$C_{11}C_{22} - C_{12}^2 > 0,$$

$$C_{11}C_{22}C_{33} + 2C_{12}C_{13}C_{23} - C_{11}C_{23}^2 - C_{22}C_{13}^2 - C_{33}C_{12}^2 > 0.$$

Since the above conditions are fulfilled by the elastic constants of $(UO_2)(O_2)(H_2O)_2$ reported in Table 1, the mechanical stability of metastudtite can be inferred.

As shown in Table 1 for $(UO_2)(O_2)(H_2O)_2{\cdot}2H_2O$, C_{33} (*c* direction) is significantly larger than the other longitudinal elastic constants C_{11} (*a* direction) and C_{22} (*b* direction). These results suggest that thermal expansion of the material will occur predominantly along the directions perpendicular to the $(UO_2)(O_2)(H_2O)_2{\cdot}2H_2O$ chains (propagating along the *c* direction). A similar conclusion can be drawn for $(UO_2)(O_2)(H_2O)_2$, since C_{11} corresponding to the *a* direction of the chains propagation is over twice larger than C_{22} and C_{33}.

The Cauchy pressure term, $C_{12} - C_{44}$, which was suggested as a standard indicator of the angular character of atomic bonding, can also be related to the brittle/ductile properties of crystals.[47] Positive values of the Cauchy pressure are typically indicative of metallic bonding, while negative values correspond to directional bonding with angular character. The Cauchy pressure is positive for both $(UO_2)(O_2)(H_2O)_2{\cdot}2H_2O$ (+12.8 GPa) and $(UO_2)(O_2)(H_2O)_2$ (+6.8 GPa), thus indicating that metallic bonding is predominant. The decrease in Cauchy pressure from $(UO_2)(O_2)(H_2O)_2{\cdot}2H_2O$ to $(UO_2)(O_2)(H_2O)_2$ reflects the increase in directional hydrogen bonding between adjacent chains as interstitial water molecules are removed upon dehydration, resulting in a crystal density increase from $\rho = 3.733$ g.cm^{-3} for $(UO_2)(O_2)(H_2O)_2{\cdot}2H_2O$ to 4.666 g.cm^{-3} for $(UO_2)(O_2)(H_2O)_2$.

The Voigt[48] approximation was used to compute the isotropic elastic properties of $(UO_2)(O_2)(H_2O)_2{\cdot}2H_2O$ and $(UO_2)(O_2)(H_2O)_2$ polycrystalline aggregates. In the method proposed by Voigt for calculating the elastic moduli, the strain throughout the aggregate of crystals is considered uniform and averaging, over all possible lattice orientations, of the relations expressing the stress is carried out.

The bulk and shear moduli by the Voigt approximation, K_V and G_V, respectively, were calculated for both monoclinic $(UO_2)(O_2)(H_2O)_2{\cdot}2H_2O$ and orthorhombic $(UO_2)(O_2)(H_2O)_2$ polycrystalline aggregates using the formulas:

$$K_V = \frac{C_{11} + C_{22} + C_{33} + 2(C_{12} + C_{13} + C_{23})}{9}$$

and

$$G_V = \frac{C_{11} + C_{22} + C_{33} - C_{12} - C_{13} - C_{23} + 3(C_{44} + C_{55} + C_{66})}{15},$$

with the C_{ij} elastic constants of Table 1. Transformation of $(UO_2)(O_2)(H_2O)_2{\cdot}2H_2O$ into $(UO_2)(O_2)(H_2O)_2$ is accompanied by an increase in K_V from 34.7 to 44.2 GPa and in G_V from 15.4 to 16.9 GPa.

While the strain is assumed to be uniform throughout the aggregate of crystals in Voigt's method, the approximation formulated by Reuss[49] considers the stress to be uniform and averaging of the relations expressing the strain is carried out. The Reuss methodology was also used to compute the isotropic elastic properties of $(UO_2)(O_2)(H_2O)_2{\cdot}2H_2O$ and $(UO_2)(O_2)(H_2O)_2$ polycrystalline aggregates.

The bulk and shear moduli within the Reuss approximation, K_R and G_R, respectively, were obtained for monoclinic $(UO_2)(O_2)(H_2O)_2{\cdot}2H_2O$ using the expressions:[43]

$$\begin{aligned} K_R = \Omega[a(C_{11} + C_{22} - 2C_{12}) + b(2C_{12} - 2C_{11} - C_{23}) \\ + c(C_{15} - 2C_{25}) \\ + d(2C_{12} + 2C_{23} - C_{13} - 2C_{22}) \\ + 2e(C_{25} - C_{15}) + f]^{-1} \end{aligned}$$

and

$$G_R = 15\{4[a(C_{11} + C_{22} + C_{12}) + b(C_{11} - C_{12} - C_{23}) + c(C_{15} + C_{25}) + d(C_{22} - C_{12} - C_{23} - C_{13}) + e(C_{15} - C_{25}) + f]/\Omega + 3[g/\Omega + (C_{44} + C_{66})/(C_{44}C_{66} - C_{46}^2)]\}^{-1},$$

where

$$\Omega = 2[C_{15}C_{25}(C_{33}C_{12} - C_{13}C_{23}) + C_{15}C_{35}(C_{22}C_{13} - C_{12}C_{23}) + C_{25}C_{35}(C_{11}C_{23} - C_{12}C_{13})] - [C_{15}^2(C_{22}C_{33} - C_{23}^2) + C_{25}^2(C_{11}C_{33} - C_{13}^2) + C_{35}^2(C_{11}C_{22} - C_{12}^2)] + gC_{55},$$

$$a = C_{33}C_{55} - C_{35}^2,$$

$$b = C_{23}C_{55} - C_{25}C_{35},$$

$$c = C_{13}C_{35} - C_{15}C_{33},$$

$$d = C_{13}C_{55} - C_{15}C_{35},$$

$$e = C_{13}C_{25} - C_{15}C_{23},$$

$$f = C_{11}(C_{22}C_{55} - C_{25}^2) - C_{12}(C_{12}C_{55} - C_{15}C_{25}) + C_{15}(C_{12}C_{25} - C_{15}C_{22}) + C_{25}(C_{23}C_{35} - C_{25}C_{33}),$$

and g as defined previously. The bulk and shear moduli for $(UO_2)(O_2)(H_2O)_2{\cdot}2H_2O$ calculated within the Reuss approximation are 25.8 and 11.3 GPa, respectively.

For polycrystalline aggregates of orthorhombic $(UO_2)(O_2)(H_2O)_2$, the Reuss bulk and shear moduli were calculated as follows:

$$K_R = \Delta[C_{11}(C_{22} + C_{33} - 2C_{23}) + C_{22}(C_{33} - 2C_{13}) - 2C_{33}C_{12} + C_{12}(2C_{23} - C_{12}) + C_{13}(2C_{12} - C_{13}) + C_{23}(2C_{13} - C_{23})]^{-1}$$

and

$$G_R = 15\{4[C_{11}(C_{22} + C_{33} + C_{23}) + C_{22}(C_{33} + C_{13}) + C_{33}C_{12} - C_{12}(C_{23} + C_{12}) - C_{13}(C_{12} + C_{13}) - C_{23}(C_{13} + C_{23})]/\Delta + 3[C_{44}^{-1} + C_{55}^{-1} + C_{66}^{-1}]\}^{-1}$$

where

$$\Delta = C_{13}(C_{12}C_{23} - C_{13}C_{22}) + C_{23}(C_{12}C_{13} - C_{23}C_{11}) + C_{33}(C_{11}C_{22} - C_{12}^2).$$

Consistent with the results obtained with Voigt's method, bulk and shear moduli for $(UO_2)(O_2)(H_2O)_2$ computed within the Reuss approximation, i.e. $K_R = 39.3$ GPa and $G_R = 13.4$ GPa, are larger than their counterparts for $(UO_2)(O_2)(H_2O)_2{\cdot}2H_2O$.

As shown by Hill[50], the Reuss and Voigt approximations result in lower and upper limits, respectively, of polycrystalline constants and practical estimates of the polycrystalline bulk and shear moduli in the Hill approximation were computed using the formulas:

$$K_H = \frac{K_R + K_V}{2}$$

and

$$G_H = \frac{G_R + G_V}{2}.$$

The bulk and shear moduli computed for $(UO_2)(O_2)(H_2O)_2{\cdot}2H_2O$ and $(UO_2)(O_2)(H_2O)_2$ are $K_H = 30.3$ GPa and $G_H = 13.4$ GPa, and $K_H = 41.8$ GPa and $G_H = 15.2$ GPa, respectively.

In the Voigt-Reuss-Hill (VRH) approximations used above, K is systematically larger than G for both $(UO_2)(O_2)(H_2O)_2{\cdot}2H_2O$ and $(UO_2)(O_2)(H_2O)_2$, which suggests that the shear modulus is the parameter limiting the mechanical stability of those crystalline structures. The ratio $R_{G/K}$ of the shear modulus divided by the bulk modulus was proposed by Pugh as a simple indicator of the correlation between the ductile/brittle properties of crystals and their elastic constants.[51] A material is considered ductile if $R_{G/K} < 0.5$, otherwise it is brittle. Therefore, according to Pugh's criteria, both $(UO_2)(O_2)(H_2O)_2{\cdot}2H_2O$ and $(UO_2)(O_2)(H_2O)_2$ are considered ductile, with ratios of $R_{G/K} = 0.44$ (with Voigt, Reuss and Hill) for $(UO_2)(O_2)(H_2O)_2{\cdot}2H_2O$, and $R_{G/K} = 0.38$ (Voigt), 0.34 (Reuss) and 0.36 (Hill) for $(UO_2)(O_2)(H_2O)_2$, the latter crystal being slightly more ductile than the former.

As discussed by Frantsevich et al.,[52] the Poisson's ratio, ν, can also be utilized to measure the malleability of crystalline compounds and is related to the Pugh's ratio given above by the relation $R_{G/K} = (3 - 6\nu)/(8 + 2\nu)$. The Poisson's ratio is close to 1/3 for ductile materials, while it is generally much less than 1/3 for brittle materials. Using the bulk and shear moduli determined above, Poisson's ratio, ν, was obtained using the expression:[43]

$$\nu = (3K - 2G)/[2(3K + G)].$$

The computed Poisson's ratio for $(UO_2)(O_2)(H_2O)_2{\cdot}2H_2O$ is 0.31 (VRH) and 0.33 (Voigt), 0.35 (Reuss) and 0.34 (Hill) for $(UO_2)(O_2)(H_2O)_2$, i.e. also pointing to a rather ductile character of these materials in the same way as the $R_{G/K}$ ratio and the Cauchy pressure term.

Young's modulus, corresponding to the ratio of the stress to strain ($E = \sigma/\varepsilon$), was computed using the formula:[44]

$$E = 9KG/(3K + G).$$

The values obtained are $E_V = 40.3$ GPa, $E_R = 29.6$ GPa, $E_H = 34.9$ GPa for $(UO_2)(O_2)(H_2O)_2{\cdot}2H_2O$ and $E_V = 45.1$ GPa, $E_R = 36.1$ GPa, $E_H = 40.6$ GPa for $(UO_2)(O_2)(H_2O)_2$. Alternatively, the axial components of Young's modulus, were derived from the elastic compliances, with its components along the *a*, *b*, and *c* directions expressed as $E_x = S_{11}^{-1}$, $E_y = S_{22}^{-1}$, and $E_z = S_{33}^{-1}$. The elastic compliances, S_{ij}, can be readily obtained by inverting the elastic constant tensor, i.e. $S = C^{-1}$. Young's modulus along the *c* direction of the chain propagation in $(UO_2)(O_2)(H_2O)_2{\cdot}2H_2O$, i.e. $E_z = 60.6$ GPa, is much stiffer than in directions perpendicular to the chains ($E_x = 37.0$ GPa and $E_y = 22.1$ GPa). Similarly, in $(UO_2)(O_2)(H_2O)_2$, the larger Young's modulus component, $E_x = 92.6$ GPa, corresponds to the chains propagation direction (*a* direction), while components in perpendicular directions are much softer, i.e. $E_y = 34.3$ GPa and

$E_z = 24.5$ GPa.

In order to assess the elastic anisotropy of $(UO_2)(O_2)(H_2O)_2{\cdot}2H_2O$ and $(UO_2)(O_2)(H_2O)_2$, the shear anisotropic factors for the {100} (A_1), {010} (A_2), and {001} (A_3) crystallographic planes were computed using the formulas:

$$A_1 = \frac{4C_{44}}{C_{11} + C_{33} - 2C_{13}},$$
$$A_2 = \frac{4C_{55}}{C_{22} + C_{33} - 2C_{23}},$$
$$A_3 = \frac{4C_{66}}{C_{11} + C_{22} - 2C_{12}}.$$

While computed A_2 values of 1.18 and 1.05 for $(UO_2)(O_2)(H_2O)_2{\cdot}2H_2O$ and $(UO_2)(O_2)(H_2O)_2$, respectively, are close to unity and suggest nearly isotropic elastic properties in the {010} plane, the predicted values of $A_1 = 0.33$ and $A_3 = 0.89$ for $(UO_2)(O_2)(H_2O)_2{\cdot}2H_2O$ and $A_1 = 0.76$ and $A_3 = 0.43$ for $(UO_2)(O_2)(H_2O)_2$ indicate larger anisotropy in the {100} and {001} planes.

Alternatively, the percentage of anisotropy in compression and shear was obtained using:

$$A_{comp} = \frac{K_V - K_R}{K_V + K_R} \times 100,$$
$$A_{shear} = \frac{G_V - G_R}{G_V + G_R} \times 100.$$

The percentages of anisotropy in compression and shear are *ca.* 15% for $(UO_2)(O_2)(H_2O)_2{\cdot}2H_2O$ ($A_{comp} = 14.8\%$ and $A_{shear} = 15.4\%$). This anisotropic character is further reduced to $A_{comp} = 5.8\%$ and $A_{shear} = 11.6\%$ for the denser $(UO_2)(O_2)(H_2O)_2$ structure (0% representing a perfectly isotropic crystal).

In terms of the recently introduced universal anisotropy index,[53]

$$A^U = 5(G_V/G_R) + (B_V/B_R) - 6,$$

$(UO_2)(O_2)(H_2O)_2{\cdot}2H_2O$ also exhibits a larger anisotropy index of $A^U = 2.17$ than $(UO_2)(O_2)(H_2O)_2$ characterized by an index of $A^U = 1.44$ ($A^U = 0$ corresponds to a perfectly isotropic crystal).

The acoustic transverse wave velocity, v_t, and longitudinal wave velocity, v_l, of $(UO_2)(O_2)(H_2O)_2{\cdot}2H_2O$ and $(UO_2)(O_2)(H_2O)_2$ were also derived from the bulk and shear moduli using the formulas:

$$v_t = \sqrt{\frac{G}{\rho}}$$

and

$$v_l = \sqrt{\frac{3K + 4G}{3\rho}}$$

with crystal densities of $\rho = 3.733$ g.cm^{-3} for $(UO_2)(O_2)(H_2O)_2{\cdot}2H_2O$ and $\rho = 4.666$ g.cm^{-3} for $(UO_2)(O_2)(H_2O)_2$. The resulting transverse wave and longitudinal wave velocities are $v_t = 2.03$ (Voigt), 1.74 (Reuss), 1.89 km/s (Hill) and $v_l = 3.85$ (Voigt), 3.31 (Reuss), 3.59 km/s (Hill) for $(UO_2)(O_2)(H_2O)_2{\cdot}2H_2O$, and $v_t = 1.90$ (Voigt), 1.69 (Reuss), 1.80 km/s (Hill) and $v_l = 3.78$ (Voigt), 3.50 (Reuss), 3.64 km/s (Hill) for $(UO_2)(O_2)(H_2O)_2$.

Using the computed acoustic transverse and longitudinal wave velocities, the mean sound velocity, v_m, was obtained using the expression:

$$v_m = \left[\frac{1}{3}\left(\frac{2}{v_t^3} + \frac{1}{v_l^3}\right)\right]^{-\frac{1}{3}}$$

and the Debye temperature was calculated according to:

$$\theta_D = \frac{h}{k_B}\left[\frac{3n}{4\pi}\left(\frac{\mathcal{N}_A\rho}{M}\right)\right]^{\frac{1}{3}} v_m,$$

where h is Planck's constant, $k_B$is Boltzmann's constant, $\mathcal{N}_A$ is Avogadro's number, n and M are the number of atoms and molar mass per formula unit, and ρ is the crystal density. The Debye temperature is related to important properties such as the specific heat or melting temperature of crystalline structures; in particular, at relatively low temperature, θ_D calculated from elastic constants or obtained from calorimetric measurements are similar. The Debye temperatures predicted within the VRH approximation are: $\theta_D = 316.23$ (Voigt), 270.84 (Reuss), 294.41 K (Hill) for $(UO_2)(O_2)(H_2O)_2{\cdot}2H_2O$ and $\theta_D = 286.53$ (Voigt), 255.55 (Reuss), 271.50 K (Hill) for $(UO_2)(O_2)(H_2O)_2$. The Debye temperature of $(UO_2)(O_2)(H_2O)_2{\cdot}2H_2O$ is found to be slightly larger than the one of $(UO_2)(O_2)(H_2O)_2$, which suggests a higher micro-hardness of the former compared to the latter.

Conclusions

The mechanical properties and stability of studtite ($(UO_2)(O_2)(H_2O)_2{\cdot}2H_2O$) and metastudtite ($(UO_2)(O_2)(H_2O)_2$), two important corrosion phases observed on spent nuclear fuel exposed to water, have been investigated using density functional perturbation theory. While $(UO_2)(O_2)(H_2O)_2$ satisfies the *necessary* and *sufficient* Born criteria for mechanical stability of orthorhombic crystals, $(UO_2)(O_2)(H_2O)_2{\cdot}2H_2O$ is found to be mechanically metastable. Indeed, *necessary* conditions for mechanical stability of monoclinic $(UO_2)(O_2)(H_2O)_2{\cdot}2H_2O$ are fulfilled, but the generic *necessary* and *sufficient* Born criterion that all eigenvalues of the stiffness matrix be positive is not satisfied. Such mechanical metastability of $(UO_2)(O_2)(H_2O)_2{\cdot}2H_2O$ might be an underlying cause of the observed irreversibility of the dehydration transformation of studtite into metastudtite occurring at moderate temperature.

For both $(UO_2)(O_2)(H_2O)_2{\cdot}2H_2O$ and $(UO_2)(O_2)(H_2O)_2$, calculated longitudinal elastic constants suggest that thermal expansion of the material will occur predominantly along the softer directions perpendicular to the chain propagation direction. The Cauchy pressure term predicted from elastic constants is positive for $(UO_2)(O_2)(H_2O)_2{\cdot}2H_2O$ and $(UO_2)(O_2)(H_2O)_2$, thus indicating that both phases are predominantly ductile, with an increase in directional hydrogen bonding between adjacent chains in $(UO_2)(O_2)(H_2O)_2$. Corroborating this finding, Pugh's ratio and Poisson's ratio also point to a rather ductile character of these materials. Within the VRH approximations, the bulk modulus *K* is systematically larger than the shear modulus *G* for both $(UO_2)(O_2)(H_2O)_2{\cdot}2H_2O$ and $(UO_2)(O_2)(H_2O)_2$, which suggests that the shear modulus is the parameter limiting the

mechanical stability of those crystalline structures.

The shear anisotropic factors for the {100}, {010} and {001} crystallographic planes were also calculated. While computed elastic properties are nearly isotropic in the {010} plane, larger anisotropy is predicted in the {100} and {001} planes. The percentages of anisotropy in compression and shear are *ca*. 15% for $(UO_2)(O_2)(H_2O)_2{\cdot}2H_2O$, while this anisotropic character is reduced to $A_{comp} = 5.8\%$ and $A_{shear} = 11.6\%$ for the denser $(UO_2)(O_2)(H_2O)_2$ structure. In terms of the recently introduced universal anisotropy index, $(UO_2)(O_2)(H_2O)_2{\cdot}2H_2O$ also exhibits a larger anisotropy index than $(UO_2)(O_2)(H_2O)_2$.

The acoustic transverse, longitudinal and mean sound wave velocities of $(UO_2)(O_2)(H_2O)_2{\cdot}2H_2O$ and $(UO_2)(O_2)(H_2O)_2$ were also derived from the bulk and shear moduli and the Debye temperature was calculated. The Debye temperatures predicted within the Hill approximation are 294 K for $(UO_2)(O_2)(H_2O)_2{\cdot}2H_2O$ and 271 K for $(UO_2)(O_2)(H_2O)_2$, which suggests a slightly lower micro-hardness of metastudtite.

Acknowledgments. Funding for this work was provided by the Used Fuel Disposition Campaign of the U.S. Department of Energy's Office of Nuclear Energy. Sandia National Laboratories is a multi-program laboratory managed and operated by Sandia Corporation, a wholly owned subsidiary of Lockheed Martin Corporation, for the U.S. Department of Energy's National Nuclear Security Administration under contract DE-AC04-94AL85000.

Notes and references

[a] *Sandia National Laboratories, Albuquerque, NM 87185, USA. E-mail: pfweck@sandia.gov*
[b] *Department of Physics and Astronomy, University of Nevada Las Vegas, Las Vegas, NV 89154, USA.*
[c] *Pacific Northwest National Laboratory, Richland, WA 99352 USA.*

[1] B. McNamara, B. Hanson, B. E. Buck, *Mater. Res. Soc. Symp. Proc.*, 2003, **757**, 401.
[2] B. Hanson, B. McNamara, E. Buck, J. Friese, E. Jenson, K. Krupka, B. Arey, *Radiochim. Acta*, 2005, **93**, 159.
[3] B. McNamara, B. Hanson, E. Buck, C. Soderquist, *Radiochim. Acta*, 2005, **93**, 169.
[4] I. G. Draganic, Z. D. Draganic, *The Radiation Chemistry of Water*, Academic Press, New York, 1971.
[5] G. Sattonnay, C. Ardois, C. Corbel, J.-F. Lucchini, M.-F. Barthe, F. Garrido, D. Gosset, *J. Nucl. Mater*., 2001, **288**, 11.
[6] M. Amme, *Radiochim. Acta*, 2002, **90**, 399.
[7] K.-A. Hughes Kubatko, K. B. Helean, A. Navrotsky, P. C. Burns, *Science*, 2003, **302**, 1191.
[8] C. R. Armstrong, M. Nyman, T. Shvareva, G. E. Sigmon, P. C. Burns, A. Navrotsky, *Proc. Natl. Acad. Sci. USA*, 2012, **109**, 1874.
[9] P. C. Burns, R. C. Ewing, A. Navrotsky, *Science*, 2012, **335**, 1184.
[10] J. F. Vaes, *Soc. Geol. Belgique Ann.*, 1947, **70**, B212.
[11] K. Walenta, *Am. Mineral.*, 1974, **59**, 166.
[12] P. C. Burns, K.-A. Hugues, *Am. Mineral.*, 2003, 88, 1165.
[13] M. Deliens, P. Piret, *Am. Mineral.*, 1983, **68**, 456.
[14] W. H. Zachariasen, CK-1367, 1944.
[15] R. Ukazi, *J. Atom. Engy. Soc. Japan*, 1959, **1**, 405.
[16] P. C. Debets, *J. Inorg. Nucl. Chem*., 1963, **25**, 727.
[17] S. Ostanin, P. Zeller, *Phys. Rev.* B, 2007, **75**, 073101.
[18] P. F. Weck, E. Kim, C. F. Jové-Colón, D. C. Sassani, *Dalton Trans.,* 2012*,* **41**, 9748.
[19] M. A. Rodriguez, P. F. Weck, J. D. Sugar, T. J. Kulp, 2015 ICDD Spring Meetings, 23-27 March 2015, ICDD Headquarters; www.icdd.com/profile/march15files/posters/Rodriguez_abstract.pdf
[20] X. Guo, S.V. Ushakov, S. Labs, H. Curtius, D. Boshbach, A. Navrotsky*, Proc. Natl. Acad. Sci. U.S.A*., 2014, **111**, 17737.
[21] T. Sato, *Naturwissenschaften*, 1961, **48**, 668, 693.
[22] E. H. P. Cordfunke, A. A. van der Diessen, *J. Inorg. Nucl. Chem*., 1963, **25**, 553.
[23] E. H. P. Cordfunke, P. Aling, *Rec. Trav. Chim. Pays-Bas,* 1963, **82**, 257.
[24] A. Rey, I. Casas, J. Gimenez, J. Quinones, J. de Pablo, *J. Nucl. Mater*., 2009, 385, 467.
[25] S. Meca, A. Martinez-Torrents, V. Marti, J. Gimenez, I. Casas, J. de Pablo, *Dalton Trans*., 2011, **40**, 7976.
[26] C. Mallon, A. Walshe, R. J. Forster, T. E. Keyes, R. J. Barker, *Inorg. Chem*., 2012, **51**, 8509.
[27] J. Gimenez, J. de Pablo, I. Casas, X. Martinez-Llado, M. Rovira, A. Martinez-Torrents, *Appl. Geochem*., 2014, **49**, 42.
[28] G. Kresse, J. Furthmüller, *Phys. Rev.* B, 1996, **54**, 11169.
[29] J. P. Perdew, K. Burke, M. Ernzerhof , *Phys. Rev. Lett.*, 1996, **77**, 3865.
[30] P. F. Weck, E. Kim, B. Masci, P. Thuery, K. R. Czerwinski, *Inorg. Chem*., 2010, **49**, 1465.
[31] P. F. Weck, C.-M. S. Gong, E. Kim, P. Thuery, K. R. Czerwinski, *Dalton Trans.*, 2011, **40**, 6007.
[32] P. F. Weck, E. Kim, C. F. Jové-Colón, D. C. Sassani, *Dalton Trans.,* 2013*,* **42**, 4570.
[33] P. F. Weck, E. Kim, *Dalton Trans.*, 2014, **43**, 17191.
[34] P. E. Blöchl, *Phys. Rev.* B, 1994, **50**, 17953.
[35] G. Kresse, D. Joubert, *Phys. Rev.* B, 1999, **59**, 1758.
[36] E. R. Davidson, *Methods in Computational Molecular Physics*, G. H. F. Diercksen and S. Wilson, Eds., Vol. 113, NATO Advanced Study Institute, Series C, Plenum, New York, 1983, p. 95.
[37] M. Methfessel, A. T. Paxton, *Phys. Rev.* B, 1989, **40**, 3616.
[38] H. J. Monkhorst, J. D. Pack, *Phys. Rev.* B, 1976, **13**, 5188.
[39] Y. Le Page, P. Saxe, *Phys. Rev.* B, 2002, **65**, 104104.
[40] J. F. Nye, *The Physical Properties of Crystals: Their Representation by Tensors and Matrices,* Oxford University Press, New York, 1985.
[41] M. Born, *Math. Proc. Cambridge Philos. Soc.*, 1940, **36**, 160.
[42] M. Born, K. Huang, *Dynamics Theory of Crystal Lattices,* Oxford University Press, Oxford, 1954.
[43] Z. J. Wu, E. J. Zhao, H. P. Xiang, X. F. Hao, X. J. Liu, J. Meng, *Phys. Rev. B*, 2007, **76**, 054115.
[44] F. I. Fedorov, *Theory of Elastic Waves in Crystals,* Springer, Berlin, 1968.
[45] J. P. Watt, *J. Appl. Phys*., 1980, **51**, 1520.
[46] F. Mouhat, F.-X. Coudert, *Phys. Rev. B*, 2014, **90**, 224104.
[47] D. G. Pettifor, *Mater. Sci. Technol.*, 1992, **8**, 345.
[48] W. Voigt, *Lehrbuch der Kristallphysik*, Leipzig Teubner, 962, 1928.
[49] A. Reuss, *Z. angew. Math. Mech*., 1929, **9**, 55.
[50] R. Hill, *Proc. Phys. Soc. London*, 1952, **65**, 349.
[51] S. F. Pugh, *Philos. Mag*., 1954, **45**, 823.
[52] I. N. Frantsevich, F. F. Voronov, and S. A. Bokuta, Elastic Constants and Elastic Moduli of Metals and Insulators Handbook, I. N. Frantsevich Ed., Naukova Dumka, Kiev, 1983, pp. 60-180.
[53] S. I. Ranganathan, M. Ostoja-Starzewski, *Phys. Rev. Lett*., 2008, **101**, 055504.